

## In Situ Fabrication of Polyaniline-Silver Nanocomposites using Soft Template of Sodium Alginate

Biplab Bhowmick,<sup>1</sup> Dibyendu Mondal,<sup>1</sup> Dipanwita Maity,<sup>1</sup> Md. Masud Rahaman Mollick,<sup>1</sup> Mrinal Kanti Bain,<sup>1</sup> Nirmal Kumar Bera,<sup>1</sup> Dipak Rana,<sup>2</sup> Sanatan Chattopadhyay,<sup>3</sup> Dipankar Chattopadhyay<sup>1</sup>

<sup>1</sup>Department of Polymer Science and Technology, University of Calcutta, 92 A.P.C. Road, Kolkata 700009, India

<sup>2</sup>Department of Chemical and Biological Engineering, Industrial Membrane Research Institute, University of Ottawa, 161 Louis Pasteur St., Ottawa, Ontario, K1N 6N5, Canada

<sup>3</sup>Department of Electronic Science, University of Calcutta, 92 A.P.C. Road, Kolkata 700009, India

Correspondence to: D. Chattopadhyay (E-mail: dipankar.chattopadhyay@gmail.com)

**ABSTRACT:** Polyaniline (PANI)-Ag nanocomposites were synthesized by *in situ* chemical polymerization approach using ammonium persulfate and silver nitrate as oxidant. Characterizations of nanocomposites were done by ultraviolet-visible (UV-vis), Fourier transform infrared (FTIR), X-ray diffraction (XRD), scanning electron microscopy, and transmission electron microscopy (TEM). UV-vis, XRD and FTIR analysis established the formation of PANI/Ag nanocomposites and face-centered-cubic phase of silver. PANI nanofibers were of average diameter  $\sim 30$  nm and several micrometers in length. Morphological analysis showed that the spherical-shaped silver nanoparticles decorate the surface of PANI nanofibers. Silver nanoparticles of average diameter  $\sim 5$ – $10$  nm were observed on the TEM images for the PANI-Ag nanocomposites. Such type of PANI-Ag nanocomposites can be used as bistable switches as well as memory devices. © 2013 Wiley Periodicals, Inc. *J. Appl. Polym. Sci.* 000: 000–000, 2013

**KEYWORDS:** composites; fibers; conducting polymers

Received 14 August 2012; accepted 4 February 2013; published online

DOI: 10.1002/app.39124

### INTRODUCTION

There has been a recent surge of interest in the synthesis and applications of electro active polymers incorporated with noble metal nanoparticles. These hybrid systems are expected to display synergistic properties of conjugated polymers and metal nanoparticles, making them potential candidates for applications in sensors and electrochemical devices.<sup>1–4</sup> Among various intrinsically conducting polymers, polyaniline (PANI) is exclusively used because of its reversible redox property, simple acid/base doping/dedoping character, superior environmental stability, unique electronic, optical properties, low cost, and so forth. However, inferior mechanical properties, insolubility in regular solvents and poor processability of PANI have hindered its potential applications. To prevail over such difficulties, the preparation of conventional thermoplastic-electroconductive polymer composites is a successful strategy to achieve unique properties and applications of the resultant materials.<sup>5–7</sup> Obviously, the fusion of the metal elements and PANI molecule can generate a new class of materials, nominated as metal-doped PANI compound, which enrich the property library and enlarge the application scope offered by each element individually. These

metal nanoparticles act as the conductive junctions between the polymer chains and results in an increase of the electrical conductivity of the composites.<sup>8–9</sup> As silver displays the highest electrical and thermal conductivities among all metals,<sup>10</sup> these PANI-Ag nanocomposites have attracted increased attention due to their interesting properties, such as catalysis, conductive inks, thick film pastes, and adhesives for various electronic components and sensors.<sup>11–14</sup> Generally, two methods are employed for the fabrication of PANI-metal nanocomposites. The most trivial and commonly tried synthetic route is the incorporation of metal nanoparticles into the polymer matrix. The negative aspect of this technique is the aggregation of nanoparticles that is quite hard to circumvent.<sup>15</sup> In the second approach, the metal nanoparticles, generated during polymerization, are homogeneously dispersed in the polymer matrix reducing agglomeration. The inclusion of metal nanoparticles inside polymer matrix is quite difficult and is bound to low concentrations.<sup>16</sup> Thus, the *in situ* synthesis of metal nanoparticles in the presence of a conducting polymer can allow the formation of nanoparticles in the interior of the polymer matrix while maintaining their low dispersity in the matrix and they exhibit unique properties and

are promising candidate for practical applications. So far, many brilliant efforts have been devoted to develop new methods for fabrication of PANI-Ag nanocomposites in different systems. For instance, Sonawane and coworkers<sup>17</sup> synthesized PANI/Ag nanocomposites by ultrasound assisted *in situ* miniemulsion polymerization. The method was found to be effective for controlled polymerization. Presence of ultrasound effectively enhances dispersion ability of silver nanoparticles of size  $\sim 10$  nm in polymer matrix. Sensitivity of fabricated device shows good reproducibility and stability of response. Response time of sensor decreases with increase in loading of Ag nanoparticles. Zarkin and coworkers<sup>18</sup> developed a novel route for synthesis of dodecanethiol-capped silver nanoparticles/PANI nanocomposites, based on a two-phase polymerization route. They noticed that the polymerization took place at the water/toluene interface, and that the silver nanoparticles are carried out to the forming polymer, resulting in a PANI mass in which the silver nanoparticles are homogeneously dispersed. In another approach sulfonated PANI-silver (SPANi-Ag) hybrid nanocomposites have been synthesized by the *in situ* reduction using a UV-curing polymerization method without using any reducing or binding agent.<sup>19</sup> Characterization of the molecular structure of the SPANi-Ag composites indicated that silver is reduced without using any reducing agent; and the metal is encapsulated/glued in the cores/surfaces of the growing polymer chains, resulting in the formation of SPANi-Ag hybrid materials. PANI-Ag nanocomposite films are fabricated via chronopotentiometry in two kinds of microemulsion systems consisting of ionic liquids (IL) and water.<sup>20</sup> It was done simultaneously by oxidative polymerization of aniline to PANI and reduction of silver nitrate to Ag nanoparticles. The PANI-Ag nanocomposites were obtained in two microemulsion systems exhibit different morphologies and properties. The PANI-Ag nanocomposite prepared in W/IL microemulsion is nanofibrous and the diameter of Ag nanocrystals is 5 nm, while the PANI-Ag nanocomposite prepared in IL/W microemulsion exhibits dendritic structure and the dispersed Ag nanoparticles have a diameter about 50–100 nm. Choudhury<sup>21</sup> successfully synthesized uniform dispersion of the spherically shaped Ag nanoparticles in the PANI matrix by *in situ* chemical polymerization approach at different Ag concentrations. The PANI/Ag nanocomposites exhibit remarkable improvement of electrical conductivity and dielectric properties when compared with pure PANI. The AC conductivity of PANI/Ag nanocomposites was increased by two orders of magnitude with respect to pure PANI. In contrast to pure PANI sensor, the PANI/Ag based sensor responded rapidly and reversibly in the presence of ethanol. A single-step process for the synthesis of silver nanoparticle- PANI derivative nanocomposites doped with poly(styrene sulphonic acid) is developed by Joyce and coworkers.<sup>22</sup> In this approach, silver nanoparticles are formed simultaneously during the polymerization process results in a good dispersion of the nanoparticles in the conductive polymer matrix. PANI-Ag nanocomposites have been synthesized through interfacial polymerization method using dimeraniline as starting material instead of aniline in presence

of aqueous solution of  $\text{AgNO}_3$  as oxidizing agent.<sup>23</sup> This work demonstrates the *in situ* nucleation and growth of PANI onto colloidal metallic surfaces. No external oxidizing agent and capping agent is used to stabilize the silver nanoparticles. Gong and coworkers<sup>24</sup> successfully prepared Ag/PANI composite nanotubes by a self-assembly polymerization process using ammonium persulfate and silver nitrate as oxidant. They proposed that the dispersed Ag nanoparticles decorated the surface of the PANI nanotubes. Stejskal and coworkers<sup>25</sup> synthesized PANI-Ag nanocomposites where Silver nitrate oxidizes aniline in the solutions of nitric acid to conducting nanofibrillar PANI. They proposed that the oxidation proceeds more easily at higher concentration of aniline but only nitric acid is present in molar excess with respect to aniline. Khanna et al.<sup>26</sup> reported the synthesis of Ag/PANI nanocomposites via *in situ* photo-redox mechanism by which radiation from UV lamps was used to reduce silver salt in aniline. Kang et al.<sup>27</sup> prepared nanocomposites by oxidative polymerization of aniline-stabilized Ag colloids by  $\gamma$ -irradiation. Core-shell silver nanocomposites using *in situ* gamma radiation-induced chemical polymerization was synthesized by Karim et al.<sup>28</sup> Du et al.<sup>29</sup> employed one-pot synthesis method for Ag/PANI nanocomposites; whereas Pillalamarri et al.<sup>30</sup> also used one-pot synthesis method in which composite materials consisting of PANI nanofibres decorated with noble-metal (Ag or Au) nanoparticles were synthesized with  $\gamma$ -radiolysis. Zhou et al.<sup>31</sup> applied the unsymmetrical square wave current method, which was characterized by the combination of an anodic process of aniline monomer polymerization and a cathodic process of metal ionic electrodeposition to produce the PANI silver nanocomposite film. Blinova et al.<sup>32</sup> produced PANI-Ag nanocomposites by the oxidation of aniline with silver nitrate in acetic acid medium. The morphology of the oxidation products includes PANI nanotubes, brushes constituted by nanowires, as well as other objects. Silver is present mainly in clusters of particles having a size of 30–50 nm, nanowires or nanorods coated with PANI, and a marble-like texture decorating some objects.

In this manuscript we detail the facile *in situ* synthesis of nanocomposites containing PANI nanofibers decorated with silver nanoparticles. This approach extends our previous work, where we illustrated that the PANI nanofibers could be formed using soft template of sodium alginate.<sup>33</sup> The presence of water-soluble metal salt in the parent solution does not alter the nanofibrillar morphology and favors the synthesis of metal nanoparticles that garnish the PANI nanofibers. Our method has several advantages over different existing techniques. This synthesis does not have the hazards of removal of hard templates, nor does it demand large amounts of organic solvents (as in interfacial polymerization)<sup>34</sup> or preformed nanofiber seeds (as in the nanofiber seeding method).<sup>35</sup> Because of its easily controllable reaction conditions and the relatively abundant reactant sources, the so-called soft chemical route, might provide an attractive option for large-scale production of nano- and micro-materials with special morphologies.<sup>36,37</sup> The beauty of our approach is that sodium alginate in the presence of protonic acid like HCl transforms into gel that governs the synthesis of PANI

nanofibers and the metal salt present in the reaction medium produces metal nanoparticles *in situ*, which decorate the nanofibers. The resulting nanocomposites have been characterized using ultraviolet–visible (UV–vis) spectroscopy; Fourier transform infrared spectroscopy (FTIR), X-ray diffraction (XRD), scanning electron microscopy (SEM), transmission electron microscopy (TEM).

## EXPERIMENTAL

### Materials

Aniline was purchased from Merck and vacuum distilled to obtain a colorless liquid. All other reagents were of analytical grade and used as received from Merck. Sodium alginate used as template was bought from Central Drug House Pvt., Delhi, India.

### Preparation of PANI-Ag Nanocomposite

A homogeneous solution of 2% sodium alginate was prepared in double distilled water. Required amount of aniline (0.25 mL) followed by 5 mL  $10^{-2}$  (M)  $\text{AgNO}_3$  were added to the alginate solution with vigorous stirring. The addition of 1 (M) HCl (4.42 mL) to the mixture transformed the solution into gel. The gelation process took several minutes to completion. Finally, solid ammonium peroxydisulfate (APS) (0.6252 g) was added to the gel and the polymerization was started instantly. The total volume of the reaction mixture is 50 mL and the concentration of  $\text{AgNO}_3$  becomes  $10^{-3}$  (M) in the final reaction mixture. The mole ratio of aniline: APS was maintained at 1 : 1. To complete the polymerization, the whole system was kept at 4°C for 24 h. The whole mass became green at the end of the polymerization.

The PANI-Ag nanocomposites were separated from the alginate gel by degelling with 1 (M) ammonium hydroxide and during degelling emeraldine salt was converted into emeraldine base form. It is understandable that HCl reacts with silver nitrate to give insoluble silver chloride in the course of the reaction which in turn forms a water-soluble complex with ammonium hydroxide. The synthesized nanocomposite was washed with distilled water to eliminate the impurities to obtain the pure nanocomposite. Finally the dedoped nanocomposites were subjected to centrifugation and then the collected residue was redoped with HCl and directed for characterization.

### Characterization

**Morphological Analysis.** TEM of synthesized nanocomposites was performed on a HRTEM (model: JEM 2010 EM) at 80 kV accelerated voltage. SEM was performed on a HITACHI-SC400N scanning electron microscope at an accelerated voltage of 15 kV.

**XRD Spectroscopy.** The XRD of PANI-Ag nanocomposites were performed with the help of a Scifert XRD 3000P diffractometer. Powder sample was taken for the structural characterization.

**UV-Vis Spectroscopy.** Absorbance spectra from 200 to 800 nm were obtained on a UV-Vis spectroscopy system (Agilent 8453 Spectrophotometer) using quartz cuvettes (1 cm path length).

**FTIR Spectroscopy.** The FTIR spectra of dried PANI-Ag nanocomposites were obtained using Shimadzu FTIR-8400S spectrometer in the range of 400–4000  $\text{cm}^{-1}$ .

**Current–Voltage (I–V) Relationship Study.** I–V characteristics curves of the pellet shaped nanocomposite sample were studied by applying voltage from –5 to +5 V at room temperature, and the current was measured at each applied voltage. The pellets of the samples of definite thickness were made by pressing the dried PANI-Ag composites.

## RESULTS AND DISCUSSION

### Fabrication of PANI-Silver Nanocomposites

The viability of the oxidation of aniline with silver nitrate to prepare PANI-Ag nanocomposites has been exemplified in a number of cases and nitric acid is produced in the course of reaction. This acid helps in aniline oxidation and adjusts the acidity of the medium.<sup>38</sup> HCl is responsible to construct excessive intermolecular hydrogen bonding in sodium alginate which directs the formation of PANI nanofibers. The typical oxidation of aniline with peroxydisulfate generates hydrogen atoms as protons, so the acidity gradually increases and the neutral aniline molecules become protonated to anilinium cations. When the acidity reaches the level needed for the protonation of pernigraniline intermediate, the anilinium cations participate in the growth of conducting polymer chains. The basic difference is that the oxidation of aniline with silver nitrate takes much more time compare to the oxidation with peroxydisulfate. Greater aniline concentration in the reaction medium neutralizes the nitric acid, which is a by-product of the oxidation. A sufficiently high acidity, needed for the successful polymerization of aniline to PANI, is thus not necessarily reached in most experiments carried out at high aniline concentration. Basically, the reaction intermediate aniline dimer is responsible for the reduction of silver nitrate as the oxidation potential of aniline dimer (+0.5V vs. SCE) is less than that of aniline (+0.8V vs. SCE). This type of metal complex catalyzed oxidation of aniline is considered to be an environmentally benign approach for the large-scale production of PANI.<sup>39</sup> Some of the recent studies reveal that the formation of nanofibers are due to the self assembly of individual polymer molecules or oligomers through  $\pi$ – $\pi$  interaction, hydrogen bonding and Van der Waals forces between aniline oligomers which causes the formation of polymeric nanofibers.<sup>40</sup>

### Morphological and Structural Analysis of PANI-Ag Nanocomposites

To investigate the morphology of as-synthesized PANI-Ag nanocomposites, microscopic analysis has been performed. The aqueous dispersion of synthesized nanocomposites is used for this purpose. Figures 1 and 2 represent the morphology of PANI-Ag nanocomposite using SEM and TEM. SEM images show that the interconnected polymeric nanofibers give rise to dendritic matrix of PANI and the spherically shaped silver nanoparticles are well adhered onto the PANI nanofibers due to the strong affinity of silver for nitrogen. As can be seen in the Figure 1, the sample consists of PANI nanofibers with average diameter  $\sim$  30 nm and several micrometers in length. The silver nanoparticles of average diameter  $\sim$  5–10 nm are observed on the TEM images for the PANI-Ag nanocomposites. The particles are not clearly monodispersed. The formation of relatively large particles with higher size dispersity could be attributed to the silver

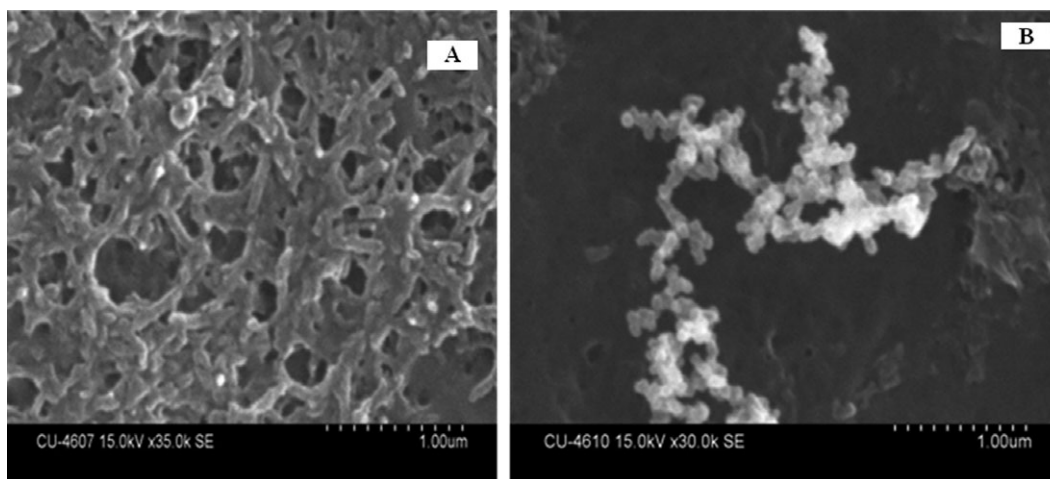


**Figure 1.** A: SEM micrographs of PANI-Ag nanocomposites. B: Magnified SEM micrographs of PANI-Ag nanocomposites.

migration and aggregation. The migration and aggregation of silver particles might be driven by the instability of silver atoms due to their high surface energy. Their aggregation would produce thermodynamically stable clusters.<sup>41,42</sup> The mechanism of the morphology formation could be described by the “secondary growth.”<sup>43</sup> It is known that the generation of PANI nanofibers is mainly affected by the secondary growth of PANI. The methods like “rapid mixing” and “interface” polymerization that prevent the secondary growth often lead to PANI nanofibers. In this reaction system, the polymerization reaction of aniline resembled template-free polymerization that lead to the formation of PANI nanofibers.

The crystalline nature of the synthesized nanocomposite is determined from XRD analysis. Figure 3 shows the XRD pattern of the corresponding nanocomposite with silver nanoparticles. The characteristic Bragg diffraction peaks for silver with  $2\theta$  of  $38.19^\circ$ ,  $44.4^\circ$ ,  $64.6^\circ$ , and  $77.6^\circ$  can be seen in the XRD patterns of the nanocomposite which corresponds to the face-centered cubic phase of silver (111), (200), (220), and (311), respectively.<sup>44</sup> The sharp patterns of diffractions clearly indicate the existence of silver nanoparticles in the composites and their crystalline nature. XRD confirms that the silver nanoparticles are immobilized within the polymer matrix. There is no specific peak at  $2\theta = 13^\circ$  for sodium alginate in the XRD pattern,<sup>45</sup> so we can conclude that there is no residual sodium alginate in the

final nanocomposite sample. Some broadening of the peaks suggests the presence of smaller sized silver nanoparticles. Two peaks at  $19.3^\circ$  and  $25.9^\circ$  are also observed, which corresponds to the distance of crystal planes of 4.6 and 3.5 Å, and could be assigned to the periodical length in the direction parallel and perpendicular to the PANI chains, respectively.<sup>46</sup> All the XRD data support the formation of PANI-Ag nanocomposite.

#### Optical and FTIR Analysis of PANI-Ag Nanocomposites

The UV-vis absorption spectrum of PANI-Ag nanocomposite is depicted in Figure 4. UV-vis is performed using sonicated dispersion of PANI-Ag nanocomposites in aqueous medium. The absorption spectra of PANI-Ag nanocomposites shows two characteristic peaks at around 320 and 608 nm which are illustrated peaks of PANI emeraldine base and could be assigned to the  $\pi$ - $\pi^*$  transition and electron transition from benzenoid to quinoid rings respectively.<sup>47-49</sup> Typically the silver nanoparticles display a Plasmon band that is located between 400 and 520 nm depending on the particle size.<sup>50</sup> A peak that appeared at 430 nm is due to the formation of silver nanoparticles during oxidative polymerization reaction of aniline using silver nitrate as oxidizing agent. It is probably due to overlapping with stronger absorption band of PANI<sup>50</sup> and may cause the shift of the absorption maximum of emeraldine base to lower wavelengths. The peak is assigned to the surface plasmon resonance absorption of the electrons in the conducting silver bands. Excitation

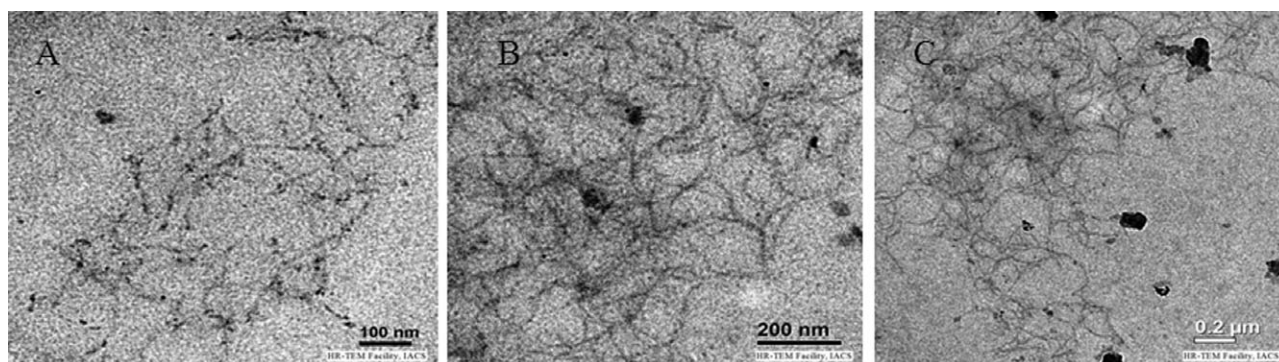


**Figure 2.** A: TEM micrographs of PANI-Ag nanocomposites. B and C: TEM micrographs of PANI-Ag nanocomposites at higher magnification.

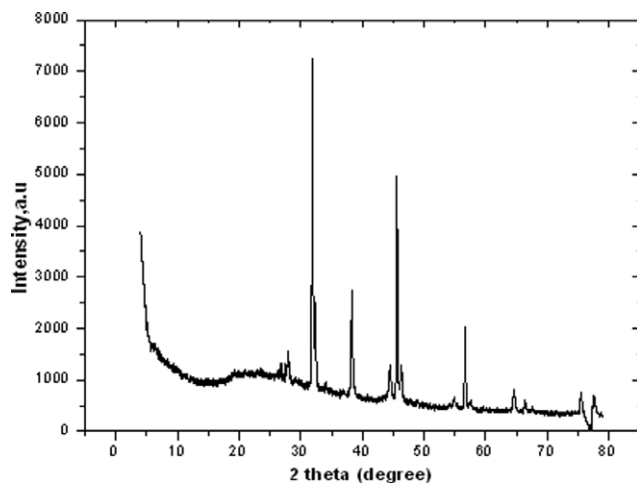


Figure 3. XRD pattern of the PANI-Ag nanocomposites.

of polymer-metal nanocomposite by the light causes induced charge density oscillation during the coupling of photons at the dielectric polymer-metal interface generates a strong absorption peak at a particular wavelength. The broad peak at 608 nm is observed due to the molecular excitation of PANI. This blue shift is for the formation of silver nanoparticles during the oxidative polymerization of aniline dimer using  $\text{AgNO}_3$  as an oxidizing agent.<sup>11</sup> However, the overall results clearly established the formation of PANI-Ag nanocomposite.

To visualize structural modifications of PANI-Ag nanocomposite, FTIR analysis is conducted at wave number region of 400–4000  $\text{cm}^{-1}$ . Figure 5 illustrates the FTIR spectra of the PANI-Ag nanocomposite. The spectra restrain relatively high absorption band in the region of stretching vibration of water molecules at about 3435  $\text{cm}^{-1}$ .<sup>21</sup> They reflect the presence of residual water in potassium bromide. The FTIR displays the peaks at 1597 and 1499  $\text{cm}^{-1}$ , which are attributed to the C=C stretching of quinoid and C=C stretching of benzoid ring respectively. We observe that there is a shift in the peaks associated with C=N and C=C stretching of quinoid ring compared to pure PANI as reported in the literature.<sup>51</sup> No appreciable change in peak posi-

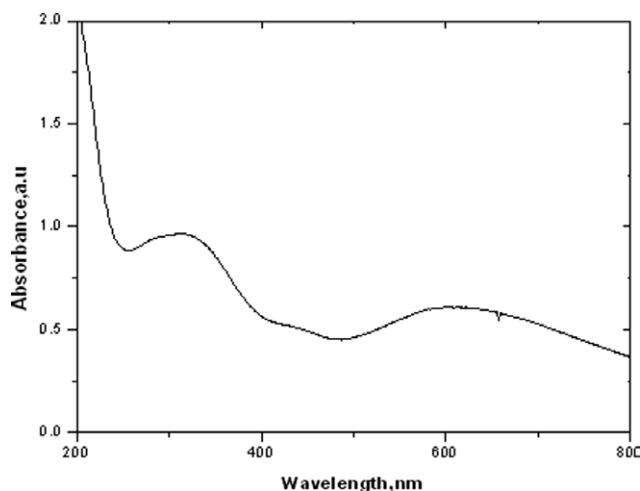


Figure 4. UV-vis spectrum of PANI-Ag nanocomposites.

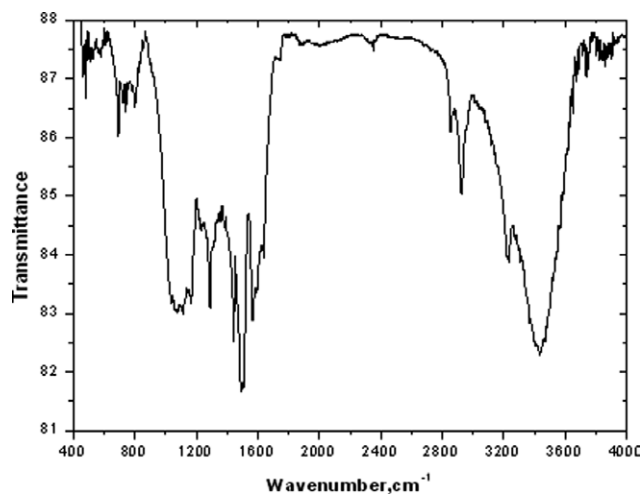


Figure 5. FTIR spectrum of PANI-Ag nanocomposites.

tion is detected for benzoid ring. So, we can conclude that silver nanoparticles may reside more close to the imine nitrogen of the PANI.<sup>51</sup> The absorption peaks around 2855 and 2931  $\text{cm}^{-1}$  correspond to C–H stretching vibrations.<sup>22</sup> The characteristic bands at 1291 and 1232  $\text{cm}^{-1}$  represent the C–N stretching vibrations of benzoid structure and the peak at 1160  $\text{cm}^{-1}$  assigns to C–H in-plane bending.<sup>50</sup> The peak at 799  $\text{cm}^{-1}$  relates to C–H bending vibration out of the plane of the para-substituted benzene rings.<sup>23</sup> The weak bands at 1444 and 1641  $\text{cm}^{-1}$  attribute to the phenazine structure of PANI.<sup>52</sup> In addition, the peak appeared at 1385  $\text{cm}^{-1}$  is due to the presence of  $\text{NO}_3^-$  ion in the nanocomposite. The insertion of anion into the PANI backbone could be achieved for the charge neutralization in the form of common ion  $\text{NO}_3^-$  during the addition of  $\text{AgNO}_3$ .<sup>53</sup> These results favor the electronic conduction in the synthesized PANI-Ag nanocomposite similar to the conduction mechanism in PANI/Au nanocomposites proposed by Tseng et al.<sup>54</sup>

#### I–V Characteristics

Figure 6 shows the plots of *I–V* characteristics of the synthesized PANI-Ag nanocomposite. *I–V* characteristic curve indicates an

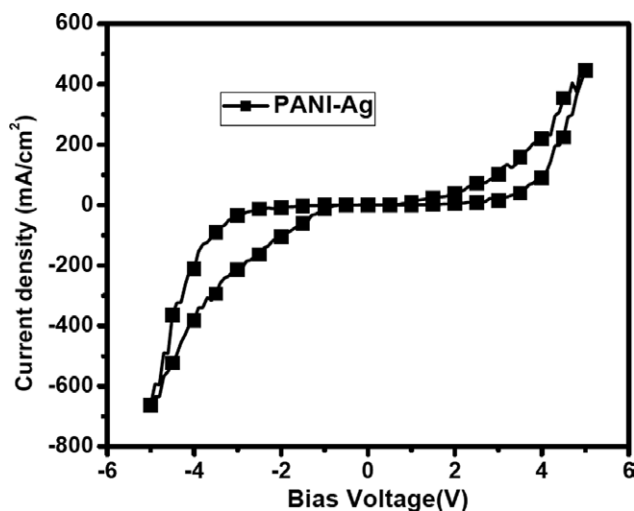
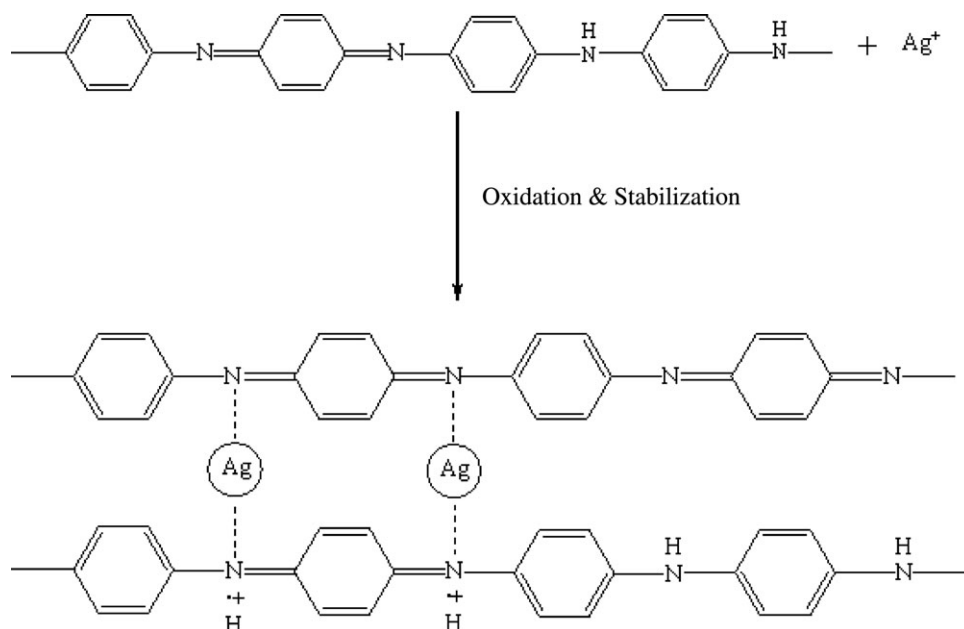


Figure 6. *I–V* characteristics of PANI-Ag nanocomposites.



**Scheme 1.** Schematic representation of interaction between PANI molecules and silver nanoparticles.

electrical bistability representing a switching behavior. This phenomenon may be termed as the switching behavior having “on” and “off” states. It is quite obvious that the current values are initially less ( $\sim 1 \mu\text{A}$ ) up to a voltage of 2.5 V and then it starts increasing and reaches to  $\sim 44 \mu\text{A}$  at 4 V. This is attributed to electronic transfer between PANI and silver nanoparticles. In the course of the reaction silver ions reduce to Ag (0) which interacts with other Ag (0) present in the surroundings to form clusters called silver nanoparticles. These Ag nanoparticles stabilize through a weak secondary bonding with PANI chains as shown in Scheme 1. Therefore, during electrical measurements such bonds are stable up to a relatively small applied voltage as 2.5 V in the present measurement. Thus up to 2.5 V the available carriers are less leading to a smaller current ( $\sim 1 \mu\text{A}$ ). When the measurement voltage increases then there is a possibility that the weak secondary bonds may break, yielding more carriers for conducting current as it is seen in Figure 6 above 2.5 V. Furthermore, the electrical measurement was performed within a cycle starting from 0 to 5 V and from 5 to 0 V in a single run. The results show that the current values from 0 to 5 V measurement cycle is higher than that in 5 to 0 V cycle at a given voltage. This is interesting since this shows a charge storing behavior in such structure. This can be explained by considering the physical rearrangement of the structure itself. It may happen that during the reduction of electric field some of the broken secondary bonds are restructured. However, not all the secondary bonds will be identical to the original structures and therefore the current is relatively less at a given voltage. Thus, this type of PANI-Ag nanocomposites can be used as bistable switches as well as memory devices.

## CONCLUSIONS

We have successfully synthesized PANI-Ag nanocomposites by *in situ* chemical polymerization approach using ammonium per-

sulfate and silver nitrate as oxidant. UV-vis, XRD, and FTIR analysis confirm the synthesis of PANI nanofibers and face-centered-cubic phase of silver. Morphological analysis shows that the dispersed and spherical shaped silver nanoparticles decorate the surface of PANI nanofibers. The *I-V* characteristics were measured to verify its applicability to develop electronic devices. The electrical study shows that such type of PANI-Ag nanocomposites are suitable to use as bistable switches and memory devices.

## ACKNOWLEDGMENTS

B. Bhowmick likes to thank the Centre for Nanoscience and Nanotechnology, University of Calcutta. D. Mondal likes to thank the Council of Scientific & Industrial Research (CSIR), Govt. of India for his fellowship, and D. Maity likes to thank the University Grant Commission, Govt. of India for her fellowship. M. M. R. Mollick likes to thank Department of Science & Technology (DST), Govt. of India for his fellowship. M.K. Bain likes to thank the University Grant Commission, Govt. of India for his fellowship under Rajiv Gandhi National Fellowship (RGNF) scheme.

## REFERENCES

1. Athawale, A. A.; Kulkarni, M. V. *Sens. Actuators B: Chem.* **2000**, *67*, 173.
2. Gao, J.; Sansiñena, J.-M.; Wang, H.-L. *Synth. Met.* **2003**, *135–136*, 809.
3. Paul, E. W.; Riccio, A. J.; Wrighton, M. S. *J. Phys. Chem.* **1985**, *89*, 1441.
4. Nohria, R.; Khillan, R. K.; Su, Y.; Dikshit, R.; Lvov, Y.; Varshramyan, K. *Sens. Actuators B: Chem.* **2006**, *114*, 218.
5. Ho, C.-H.; Liu, C.-D.; Hsieh, C.-H.; Hsieh, K.-H.; Lee, S.-N. *Synth. Met.* **2008**, *158*, 630.

6. Castillo-Ortega, M. M.; Rodríguez, D. E.; Encinas, J. C.; Plascencia, M.; Méndez-Velarde, F. A.; Olayo, R. *Sens. Actuators B: Chem.* **2002**, *85*, 19.
7. Chattopadhyay, D.; Bain, M. K. *J. Appl. Polym. Sci.* **2008**, *110*, 2849.
8. Gangopadhyay, R.; Amitabha, D. *Chem. Mater.* **2000**, *12*, 608.
9. Del Castillo-Castro, T.; Larios-Rodríguez, E.; Molina-Arenas, Z.; Castillo-Ortega, M. M.; Tanori, J. *Composites A: Appl. Sci. Manuf.* **2007**, *38*, 107.
10. Sun, Y.; Xia, Y. *Adv. Mater.* **2002**, *14*, 833.
11. Feng, X.; Mao, C.; Yang, G.; Hou, W.; Zhu, J.-J. *Langmuir* **2006**, *22*, 4384.
12. Jin, R.; Cao, Y. W.; Mirkin, C. A.; Kelly, K. L.; Schatz, G. C.; Zheng, J. G. *Science* **2001**, *294*, 1901.
13. Gould, J. R.; Lenhard, J. R.; Muentner, A. A.; Godleski, S. A.; Farid, S. *J. Am. Chem. Soc.* **2000**, *122*, 11934.
14. Li, X.; Gao, Y.; Gong, J.; Zhang, L.; Qu, L. *J. Phys. Chem. C* **2009**, *113*, 69.
15. Leroux, Y.; Eang, E.; Fave, C.; Trippe, G.; Lacroix, J. C. *Electrochem. Commun.* **2007**, *9*, 1258.
16. Kim, I.-W.; Lee, J.-E.; Ryu, J.-H.; Lee, J.-S.; Kim, S.-J.; Han, S.-H.; Chang, I.-S.; Kang, H.-H.; Suh, K.-D. *J. Polym. Sci. A: Polym. Chem.* **2004**, *42*, 2551.
17. Barkade, S. S.; Naik, J. B.; Sonawane, S. H. *Colloids Surfaces A: Physicochem. Eng. Asp.* **2011**, *378*, 94.
18. Oliveira, M. M.; Castro, E. G.; Canestraro, C. D.; Zanchet, D.; Ugarte, D.; Roman, L. S.; Zarbin, A. J. G. *J. Phys. Chem. B* **2006**, *110*, 17063.
19. Karim, M. R.; Yeum, J. H.; Lee, M.-Y.; Lee, M. S.; Lim, K. T. *Polym. Adv. Technol.* **2009**, *20*, 639.
20. Zhou, Z.; He, D.; Guo, Y.; Cui, Z.; Wang, M.; Li, G.; Yang, R. *Thin Solid Films* **2009**, *517*, 6767.
21. Choudhury, A. *Sens. Actuators B: Chem.* **2009**, *138*, 318.
22. Neelgund, G. M.; Hrehorova, E.; Joyce, M.; Bliznyuk, V. *Polym. Int.* **2008**, *57*, 1083.
23. Paulraj, P.; Janaki, N.; Sandhya, S.; Pandian, K. *Colloids Surfaces A: Physicochem. Eng. Asp.* **2011**, *377*, 28.
24. Gao, Y.; Shan, D.; Cao, F.; Gong, J.; Li, X.; Ma, H.-Y.; Su, Z.-M.; Qu, L.-Y. *J. Phys. Chem. C* **2009**, *113*, 15175.
25. Blinova, N. V.; Stejskal, J.; Trchová, M.; Sapurina, I.; Ciric-Marjanovic, G. *Polymer* **2009**, *50*, 50.
26. Khanna, P. K.; Singh, N.; Charan, S.; Kasi Viswanath, A. *Mater. Chem. Phys.* **2005**, *92*, 214.
27. Kang, Y.-O.; Choi, S.-H.; Gopalan, A.; Lee, K.-P.; Kang, H.-D.; Song, Y. S. *J. Non-Cryst. Solids* **2006**, *352*, 463.
28. Karim, M. R.; Lim, K. T.; Lee, C. J.; Bhuiyan, M. T. I.; Kim, H. J.; Park, L. S.; Lee, M. S. *J. Polym. Sci. Part A: Polym. Chem.* **2007**, *45*, 5741.
29. Du, J.; Liu, Z.; Han, B.; Li, Z.; Zhang, J.; Huang, Y. *Micropor. Mesopor. Mater.* **2005**, *84*, 254.
30. Pillalamarri, S. K.; Blum, F. D.; Tokuhira, A. T.; Bertino, M. F. *Chem. Mater.* **2005**, *17*, 5941.
31. Zhou, H. H.; Ning, X. H.; Li, S. L.; Chen, J. H.; Kuang, Y. F. *Thin Solid Films* **2006**, *510*, 164.
32. Blinova, N. V.; Bober, P.; Hromádková, J.; Trchová, M.; Stejskal, J.; Prokeš, J. *Polym. Int.* **2010**, *59*, 437.
33. Bhowmick, B.; Bain, M. K.; Maity, D.; Bera, N. K.; Mondal, D.; Mollick, Md. M. R.; Maiti, P. K.; Chattopadhyay, D. *J. Appl. Polym. Sci.* **2012**, *123*, 1630.
34. Huang, J.; Virji, S.; Weiller, B. H.; Kaner, R. B. *J. Am. Chem. Soc.* **2003**, *125*, 314.
35. Zhang, X.; Goux, W. J.; Manohar, S. K. *J. Am. Chem. Soc.* **2004**, *126*, 4502.
36. Wang, Z.; Qian, X.-F.; Yin, J.; Zhu, Z.-K. *Langmuir* **2004**, *20*, 3441.
37. Zhang, L.; Wan, M. *Adv. Funct. Mater.* **2003**, *13*, 815.
38. Bober, P.; Stejskal, J.; Trchová, M.; Hromádková, J.; Prokeš, J. *React. Funct. Polym.* **2010**, *70*, 656.
39. Mourato, A.; Correia, J. P.; Siegenthaler, H.; Abrantes, L. M. *Electrochim. Acta* **2007**, *53*, 664.
40. O'Mullane, A. P.; Dale, S. E.; Macpherson, J. V.; Unwin, P. R. *Chem. Commun.* **2004**, *14*, 1606.
41. Carotenuto, G. *Appl. Organomet. Chem.* **2001**, *15*, 344.
42. Carotenuto, G.; Marletta, G.; Nicolais, L. *J. Mater. Sci. Lett.* **2001**, *20*, 663.
43. Huang, J.; Kaner, R. B. *Angew. Chem. Int. Ed. Engl.* **2004**, *43*, 5817.
44. Chen, C.; Wang, L.; Jiang, G.; Zhou, J.; Chen, X.; Yu, H. *Nanotechnology* **2006**, *17*, 3933.
45. Kim, S.-G.; Lim, G.-T.; Jegal, J.; Lee, K.-H. *J. Membr. Sci.* **2000**, *174*, 1.
46. Pan, L. J.; Pu, L.; Shi, Y.; Sun, T.; Zhang, R.; Zheng, Y. O. *Adv. Funct. Mater.* **2006**, *16*, 1279.
47. Kulkarni, M.V.; Viswanath, A. K. *Eur. Polym. J.* **2004**, *40*, 379.
48. Kohut-Svelko, N.; Reynaud, S.; Francois, J. *Synth. Met.* **2005**, *150*, 107.
49. do Nascimento, G. M.; Constantino, V. R. L.; Landers, R.; Temperini, M. L. A. *Polymer* **2006**, *47*, 6131.
50. Ayad, M. M.; Prastomo, N.; Matsuda, A.; Stejskal, J. *Synth. Met.* **2010**, *160*, 42.
51. Afzal, A. B.; Akhtar, M. J.; Nadeem, M.; Ahmad, M.; Hassan, M. M.; Yasin, T.; Mehmood, M. *J. Phys. D: Appl. Phys.* **2009**, *42*, 015411 (8 pp).
52. Huang, Z.-H.; Shi, L.; Zhu, Q.-R.; Zou, J.-T.; Chen, T. *Chin. J. Chem. Phys.* **2010**, *23*, 701.
53. Bouazza, S.; Alonzo, V.; Hauchard, D. *Synth. Met.* **2009**, *159*, 1612.
54. Tseng, R. J.; Huang, J.; Ouyang, J.; Kaner, R. B.; Yang, Y. *Nano Lett.* **2005**, *5*, 1077.